

A Thesis Presented to  
The Faculty of the Alfred University

GROWTH OF CARBON NANOTUBES ON  
BORON CARBIDE AS A MEANS OF DISPERSION

by

Branndon R. Chen

In Partial Fulfillment of  
the Requirements for

The Alfred University Honors Program

May 2016

Alfred, New York

Under the Supervision of:

Chair:

Dr. David W. Lipke

Committee Members:

Dr. Steven M. Pilgrim

Dr. William Carlson

## Acknowledgments

First and foremost, I would like to thank my parents for their continued support. This thesis was completed with great support from my advisor Dr. David Lipke. Special thanks to Jim Thiebaud for technical support; and to Gerry Wynick for assistance with SEM imaging; as well as to Steve Conderman and Alan Rae for their help and allowing access at the Ceramics Corridor Innovation Center. Thanks also to Dr. Steven Pilgrim as well as Dr. William Carlson.

# Table of Contents

Section	Page
Acknowledgments	ii
Table of Contents	iii
I. List of Figures	iv
II. Abstract	v
III. Introduction	1
IV. Experimental	4
V. Results and Discussion	8
VI. Conclusion	16
VII.Future Work	17
VIII.References	18

# I. List of Figures

Figure	Page
Figure 1. Illustration of CNT growth mechanism, (a) tip growth and (b) base growth <sup>1</sup> (P.J.F. Harris).....	2
Figure 2. Stock boron carbide (Alfa Aesar #40504). Secondary electron (SE) image taken at 20,000x. ....	8
Figure 3. Boron carbide after growth trial; ferrocene used as catalyst precursor. SE image taken at 20,000x. ....	9
Figure 4. Boron carbide after growth trial; 1 wt% metallic iron. Arrows indicate deposited catalyst. SE image taken at 22,000x. ....	10
Figure 5. Boron carbide after growth trial; 5 wt% metallic iron. Arrows indicate deposited catalyst. SE image taken at 30,000x. ....	11
Figure 6. Boron carbide after growth trial; 3 + 1 wt% metallic iron-molybdenum. Arrows point to smaller carbon nanotube growths near the large nanotube. SE image taken at 20,000x. ....	12
Figure 7. (a)Image of boron carbide after growth trial; 3 + 1 wt% metallic iron-molybdenum. (b) Backscatter image of the same area; elemental contrast can be seen. Images taken at 20,000x. ....	12
Figure 8. Silicon wafer (a) and loose catalyst powder (b) loaded with an iron based catalyst. Growth trial occurred using the EasyTube® 2000 CVD Furnace. Arrows point to carbon nanotubes. SE images taken at 50,000x. .	14
Figure 9. Overlaid XRD plots. Silicon carbide and boron carbide peaks marked. Question marks “?” indicate peaks from an unknown phase.....	15



## II. Abstract

Carbon nanotubes (CNTs) possess many attractive properties such as high strength and modulus<sup>1</sup> that make them attractive for use as composite reinforcement. *In situ* growth of CNTs on boron carbide powder was investigated as a method for dispersing nanotubes in ceramic composites. Catalyst precursors were deposited on boron carbide powder via precipitation/co-precipitation. Successful growth of CNTs occurred using a co-precipitated iron-molybdenum catalyst; however, CNT growth was sparse. Yields were lower than previous work utilizing a similar catalyst with a different substrate<sup>2</sup>. Future work is necessary to understand the relationships between catalyst precursor and yield.

### III. Introduction

Carbon nanotubes (CNTs) have attractive properties such as high specific strength/modulus<sup>1</sup>. These properties show promise for fiber reinforcement in composites. The principle of fiber reinforcement is to transfer the load from the matrix to the fibers, as well as provide mechanisms to absorb energy as a crack propagates through the material<sup>3</sup>. Because the nanotubes are on the particle surfaces prior to consolidation, the nanotubes can bridge between the boron carbide grains in a sintered body, providing reinforcement.

For reinforcement to occur optimally, the CNTs must be uniformly distributed through the matrix material, boron carbide in this case. Good carbon-carbon covalent bonding between the boron carbide matrix and the carbon nanotubes would facilitate load transfer. In a study performed by Lao *et al.* boron was reacted with nanotubes, which formed boron carbide. They indicated that boron carbide can be bonded to CNTs<sup>4</sup>.

Transition metal nanoparticles are typically used as a catalyst to grow CNTs. The partially filled d-band electronic structure plays a critical role in catalyzing the dissociation of hydrocarbons<sup>5</sup>. Iron is the most active of the transition metals and is most commonly used<sup>1,5,6</sup>. The addition of molybdenum increases the stability the iron catalysts by reducing

aggregation; molybdenum co-catalysts promote growth and thus increase CNT yield<sup>1,2,5</sup>. Catalysts can be deposited by several methods such as sputtering, vapor transport and decomposition of metallocenes, and precipitation/co-precipitation of metal salts<sup>1,6–8</sup>.

CNT growth occurs when a hydrocarbon feedstock gas is thermally decomposed and absorbed, then precipitated on a catalyst surface. On the bottom of a catalyst particle, hydrocarbons are decomposed/absorbed; the top of the catalyst particle is where the nanotube stems and grows<sup>1</sup>. Figure 1 illustrates the mechanisms of CNT growth. Single-wall nanotubes (SWNTs)

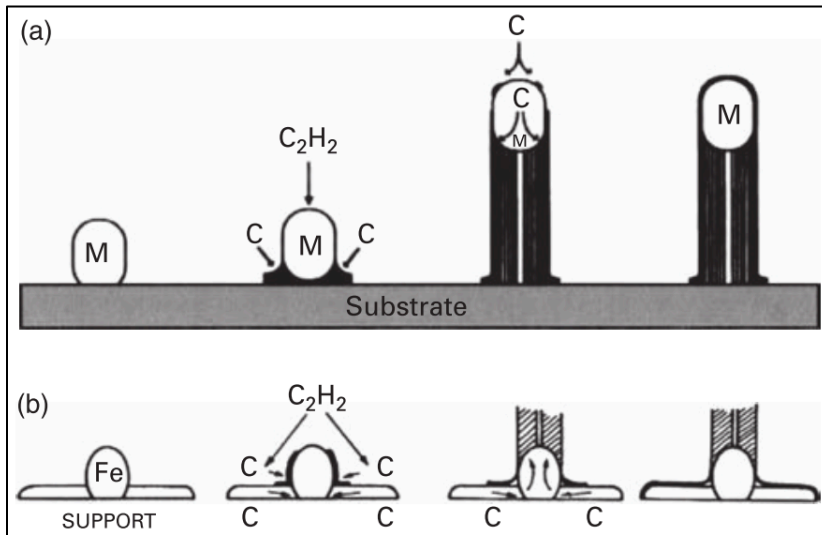


Figure 1. Illustration of CNT growth mechanism, (a) tip growth and (b) base growth<sup>1</sup> (P.J.F. Harris).

are indicative of a tip growth mechanism. Tip growth occurs when there is weak interaction between the support and catalyst particle<sup>1,5</sup>. The catalyst particles become fully saturated with carbon, which is then lifted off, in the form of a tube. SWNTs are typically formed from a single metal catalyst

particle. SWNTs have a diameter of 1-5nm<sup>1,5</sup>. Base growth occurs when the interaction between catalyst particles and support is strong. Multi-walled nanotubes (MWNTs) are much wider in diameter than SWNTs, ranging from 10-80nm in diameter<sup>1,5</sup>. Hydrocarbons are decomposed on one side of the catalyst particle surface and CNT growth occurs on the other<sup>1</sup>. Base growth occurs when carbon is added from the base of the nanotube.

A boron carbide-CNT composite material system has been previously attempted by Woodman *et al.*<sup>9</sup> Their work utilized ball milling of CNTs and boron carbide powder as a method of dispersing the CNTs. This method was ineffective as large pore structures were observed throughout the composite caused by agglomerated CNTs. Strength of the composite was significantly lower than the boron carbide containing no CNTs.

Agglomeration of CNTs is the biggest problem to overcome. The van der Waals forces between CNTs are quite strong, leading to tangled agglomeration<sup>9</sup>. Agglomerates range in size from small bunches of several nanotubes to clusters as large as 100µm in diameter<sup>1,9</sup>. Uniformly depositing catalyst and growing CNTs can minimize agglomeration. This project aims to grow CNTs on boron carbide powder as a method of dispersing the CNTs.

## IV. Experimental

### *Catalyst Deposition*

CNT catalyst precursor was deposited on boron carbide powder by two methods. One used dissolved ferrocene in toluene. The other method precipitated/co-precipitated iron hydroxide/iron-molybdenum hydroxide.

A target was set for a 0.1 wt % metallic iron based upon high expected yields of CNTs<sup>10</sup>. In a round bottom flask 0.5792 g ferrocene (Alfa Aesar #87202) was added to 60 ml toluene (Fisher Science #S25611A). Thirty grams (30 g) of boron carbide, 1-7  $\mu\text{m}$  (Alfa Aesar #40504) was added and mixed into the solution. The suspension was then placed in a Yamato RE200 Rotary Evaporator, equipped with a room temperature water bath and vacuum pump, for 1 hour until the toluene evaporated. The sample was recovered and crushed in a porcelain mortar and pestle.

A higher target of 1 wt % metallic iron was set after the ferrocene loaded trial proved unsuccessful. For these trials a modified procedure was followed: 2.172 g iron nitrate (Alfa Aesar #12229) was dissolved in 40 ml deionized water in an Erlenmeyer flask. Thirty grams (30 g) of boron carbide was added to the solution. Twenty six (26 ml) ammonium hydroxide, 28-30%, (Alfa Aesar #33285) was added drop by drop. The suspension was placed in a centrifuge set at 2600 rpm for 10 min. The supernatant was then discarded; the pellet was washed and re-suspended in ethanol. The suspension was then

placed in a recrystallization dish and dried overnight (18 hours) at 84°C. A trial with a higher target of 5 wt % metallic iron was also prepared using 11.010 g iron nitrate and 80 ml of ammonium hydroxide.

A target of 3 + 1 wt % metallic iron/molybdenum was prepared as follows. Using a round bottom flask with a stir bar, 2.24 g ferrous sulfate (Fisher Science #S25325) was dissolved in 15 ml of deionized water; 14.4 g of boron carbide was then added to the solution. In a separate beaker, 0.47 g of ammonium molybdate was dissolved in 10 ml water. The ammonium molybdate solution was added to the boron carbide suspension drop by drop. The suspension was then placed in a Yamato RE200 Rotary Evaporator, equipped with a boiling water bath and vacuum pump, for 1 hour until the water evaporated. The flask was placed in a drying oven overnight (18 hours) at 98°C. The contents were recovered and crushed using a porcelain mortar and pestle.

### *CNT Growth*

A chemical vapor deposition (CVD) furnace was used to reduce catalyst precursors and grow CNTs. The reaction chamber was evacuated by mechanical vacuum pump to hold a base pressure of 0.048 torr. Reduction occurred at 660°C while flowing 100 standard cubic centimeters per minute

(SCCM) of ammonia gas for 30 minutes; growth occurred at this same temperature while flowing 200 SCCM of acetylene gas for 45 minutes.

Similar growth conditions were evaluated using a commercially available CNT reactor, the FirstNano EasyTube® 2000 CVD Reactor, located in Room 216 of the Ceramic Corridor Innovation Center. Growth trials of CNT occurred using sputtered iron-alumina on silicon wafers as well as iron supported on a zeolite powder, both of which are industry standards. The process occurred under argon atmosphere. Once the reactor reached 720°C, the samples were inserted to the reaction chamber, H<sub>2</sub> was injected to reduce the samples for 15 minutes. Temperature was increased to 750°C; H<sub>2</sub> and ethylene were injected during the growth segment for 30 minutes. The samples were kept in a H<sub>2</sub> reducing atmosphere during cooling until 300°C, which was then switched to pure argon until room temperature unloading.

### *Microscopy*

Scanning electron microscopy was conducted using a JEOL JXA-8200. Powders were mounted to sample stages using conductive carbon tape. Samples were observed with an accelerating voltage of 2kV. Secondary electron (SE) and backscatter electron (BSE) images were recorded at various magnifications (20,000x to 50,000x).

### *Phase analysis*

X-ray diffraction (XRD) phase identification was conducted with a Bruker D2 Phaser diffractometer. XRD scanning parameters were from  $10^{\circ}$  to  $75^{\circ} 2\theta$ ; with a step size of  $0.03^{\circ} 2\theta$ ; and a step time of 0.3s. Sample powders were packed in a clean zero background holder using a microscope slide and aluminum punch to ensure the sample was flush with the top of the sample holder.



## V. Results and Discussion

### *SEM Results*

Figure 2 shows stock boron carbide. Both small and large particles are present. Figure 3 shows boron carbide loaded with ferrocene, after a decomposition and growth trial. When compared to the stock boron carbide, it is difficult to identify the presence of any iron catalyst. Ferrocene was deemed an ineffective catalyst precursor for the CVD setup.

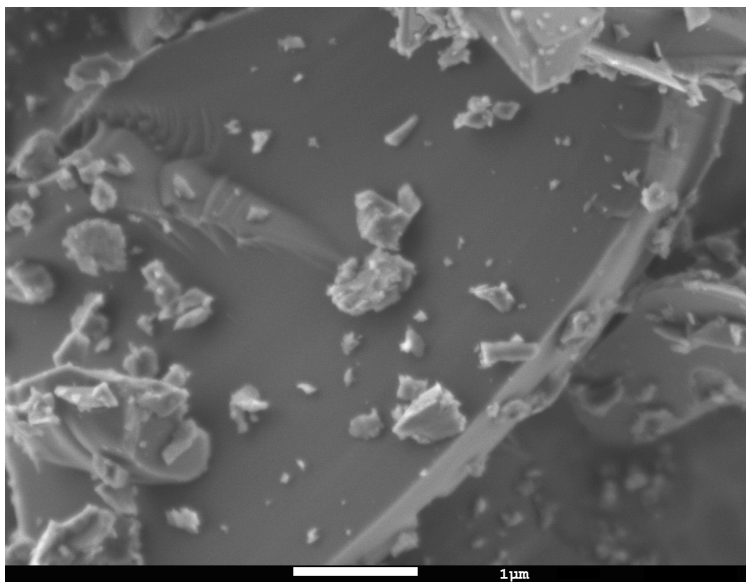


Figure 2. Stock boron carbide (Alfa Aesar #40504). Secondary electron (SE) image taken at 20,000x.

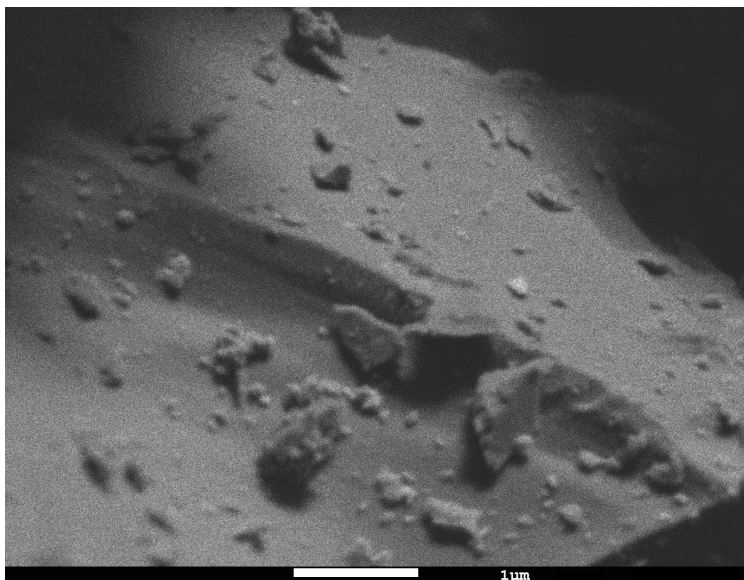


Figure 3. Boron carbide after growth trial; ferrocene used as catalyst precursor. SE image taken at 20,000x.

Iron hydroxide at 1 wt% metallic iron was precipitated using iron nitrate and ammonium hydroxide. Figure 4 shows iron precipitates along the edges of particles based on round particle morphologies. Even though the catalyst was present, no growth of CNT occurred.

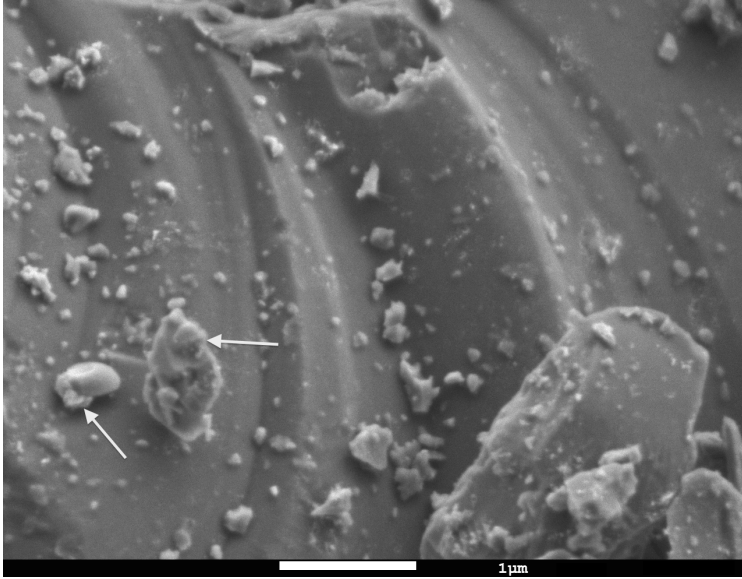


Figure 4. Boron carbide after growth trial; 1 wt% metallic iron. Arrows indicate deposited catalyst. SE image taken at 22,000x.

As discussed earlier, another trial at a higher loading of 5 wt% iron catalyst was attempted. After the reduction and growth trial, no CNT could be identified. Catalyst can be clearly seen on the boron carbide particles, see Figure 5.

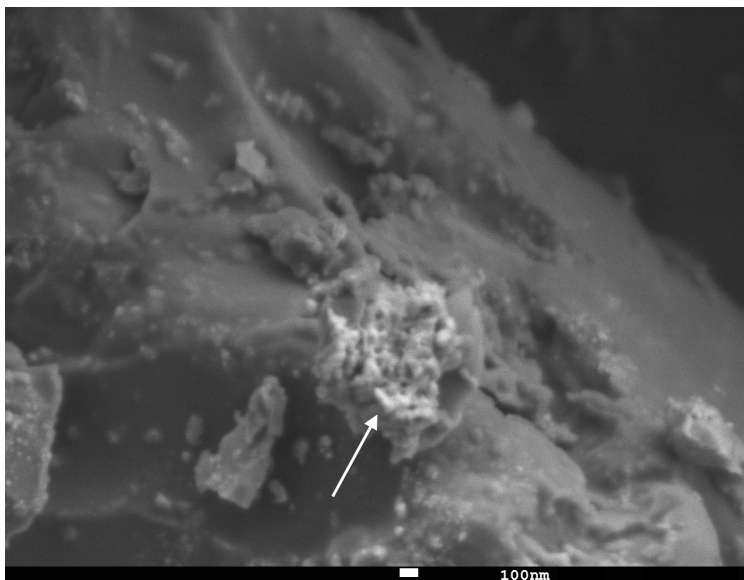


Figure 5. Boron carbide after growth trial; 5 wt% metallic iron. Arrows indicate deposited catalyst. SE image taken at 30,000x.

Figure 6 shows boron carbide after reduction and growth using a co-precipitated iron-molybdenum hydroxide catalyst precursor. There is one distinct nanotube protruding from the surface. In the surrounding area, shorter nanotubes are also present. Figure 7a shows another area where CNTs have also grown on boron carbide. A backscatter image taken to show elemental contrast between the boron carbide and iron-molybdenum catalyst particles, see Figure 7b. The distribution of catalyst can be seen along the boron carbide particle edges. On the large face of the boron carbide particle, no deposited catalyst can be seen.

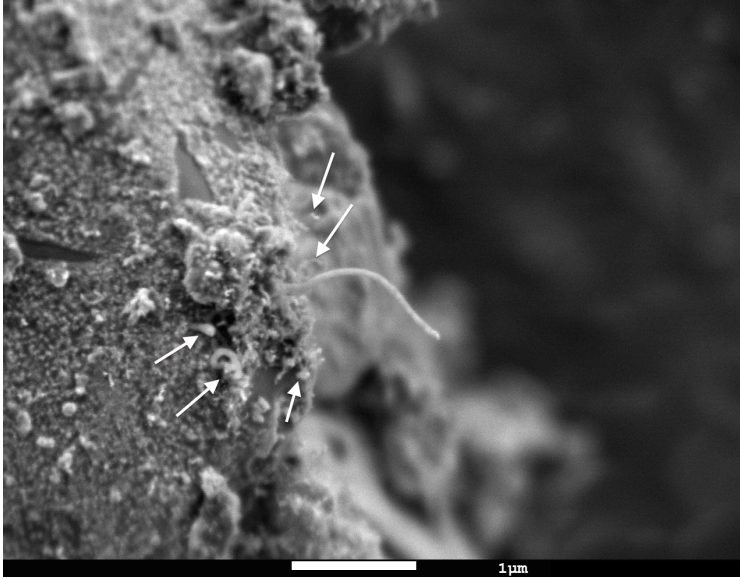
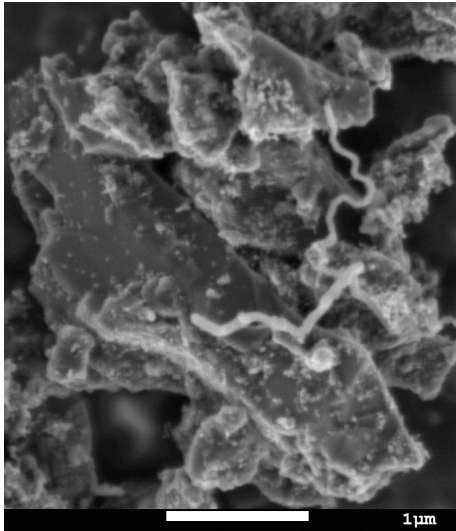
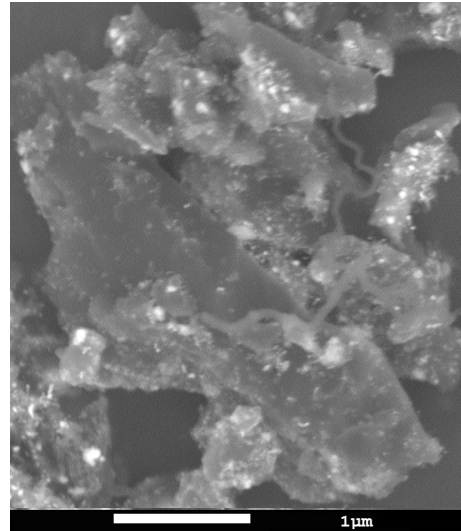


Figure 6. Boron carbide after growth trial; 3 + 1 wt% metallic iron-molybdenum. Arrows point to smaller carbon nanotube growths near the large nanotube. SE image taken at 20,000x.



(a) Secondary electron image



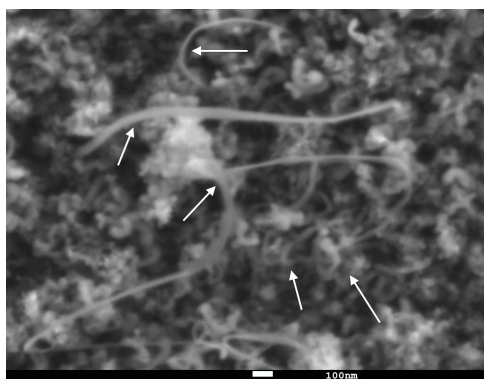
(b) Backscatter electron image

Figure 7. (a) Image of boron carbide after growth trial; 3 + 1 wt% metallic iron-molybdenum. (b) Backscatter image of the same area; elemental contrast can be seen. Images taken at 20,000x.

The co-precipitated iron-molybdenum catalyst proved successful for CNT growth, seen Figures 6, 7a, and 7b. The iron particles using both ferrocene and precipitated iron hydroxide were unsuccessful at nucleating CNT growth. The CNTs produced with the co-precipitated catalyst had a large diameter, roughly 50-80nm. A diameter of this size indicates a base growth mechanism as well as a multiwall structure. Tip growth CNTs would have a diameter closer to 5nm or less and commonly have a single-wall structure<sup>1,5</sup>. Growth was sparse; no mass was gained during growth. In contrast, 8000% weight increases have been reported for this co-precipitated catalyst on an calcium oxide substrate<sup>2</sup>. Despite the low yield, *in situ* growth of CNTs on boron carbide seems to be a viable method of dispersing nanotubes. The bond between the substrate/catalyst and the nanotube helps prevent nanotubes from agglomerating.

The pore structure of substrate materials is also thought to influence growth of CNTs<sup>5</sup>. Catalyst would preferentially deposit in the pores on the surface. The diameter of the CNT would then track the diameter of the respective pore<sup>5</sup>. In this work, boron carbide appeared to have a smooth surface and catalyst precursor preferentially deposited along the edges, a rougher surface. Consequently using boron carbide with a smaller particle size would result in a more uniform CNT distribution.

CNT growth using the silicon wafer substrate in the EasyTube® 2000 system showed no visible growth upon initial inspection. SEM imaging was required to identify the presence of CNTs; Figure 8a shows a layer of tangled nanotubes. The loose powder catalyst grown under the same conditions also required SEM imaging to identify the presence of nanotubes, see Figure 8b. Growth conditions for this system need to be refined to achieve optimal yield.



(a) Silicon wafer



(b) Loose catalyst powder

Figure 8. Silicon wafer (a) and loose catalyst powder (b) loaded with an iron based catalyst. Growth trial occurred using the EasyTube® 2000 CVD Furnace. Arrows point to carbon nanotubes. SE images taken at 50,000x.

### *XRD Results*

X-Ray diffraction indicated (Figure 9) that the stock material was not solely boron carbide; silicon carbide was present as a contaminant, most likely from processing<sup>11</sup>. Since aligned CNT arrays are grown on silicon wafers, silicon should not affect CNT growth in this system. The question marks indicate peaks of an unknown phase. Iron and molybdenum peaks, and their respective oxide and hydroxide peaks, were overlaid, but did not match the recorded sample scans.

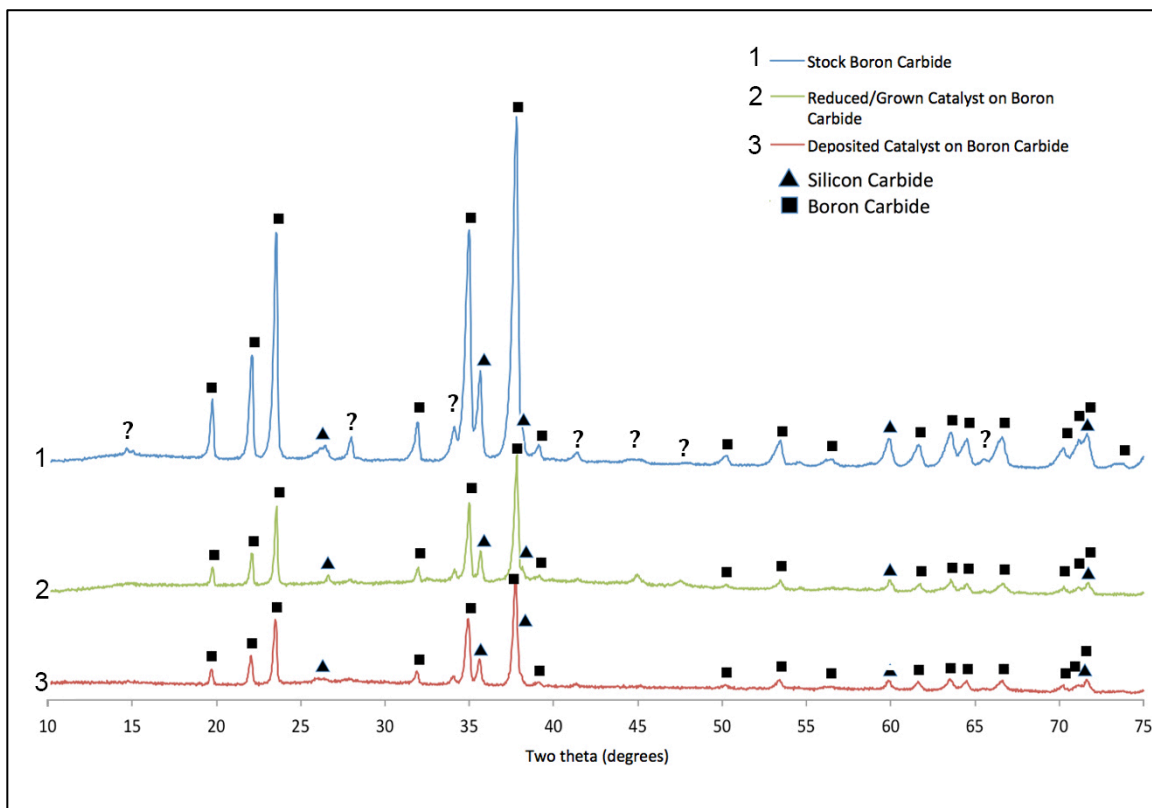


Figure 9. Overlaid XRD plots. Silicon carbide and boron carbide peaks marked. Question marks “?” indicate peaks from an unknown phase.



## VI. Conclusion

Carbon nanotubes can be grown on boron carbide powder using 3 + 1 wt% iron-molybdenum co-precipitated catalyst. Trials using iron as the catalyst did not yield carbon nanotube growth. The addition of molybdenum promoted carbon nanotube growth. *In situ* growth of CNTs on boron carbide appears to be a viable method of CNT dispersal. When compared to ball milled powder<sup>9</sup>, agglomeration of CNTs is minimized as the nanotubes are bonded to the catalyst/support material. Controlling catalyst precursor deposition, as well as the morphology and size of substrate powders need to be further investigated.

## VII. Future Work

The next step is to understand what governs CNT yield. Several approaches are possible. One is to tailor the reduction and growth parameters (time, temperature, gas flow, etc.). Another is to precipitate mono-disperse catalyst particles and deposit the particles separately. Catalyst particles can be deposited on the surface using electrolyte media or opposite charged catalyst and substrate particles; this is known as hetero-coagulation.

Based on the current samples processed using the EasyTube® 2000 CVD Furnace, further investigation is needed to determine suitable growth conditions. Process temperature, catalyst, reducing atmosphere, feedstock gas, and growth time parameters need to be determined for this system.

Once CNT yields are higher, on the order of 1-5 vol%, consolidation of a composite can be conducted using spark plasma sintering (SPS). SPS has shown better results with CNT-alumina and CNT-SiC consolidation than traditional sintering methods such as hot-pressing<sup>1</sup>.

## VIII. References

- 1 P.J.F. Harris, *Carbon Nanotube Science Synthesis, Properties and Applications*. Cambridge University Press, 2009.
- 2 R. Rajarao and B.R. Bhat, "High Yield Synthesis of Carbon Nanotubes on Easy Soluble Support," **2** [3] 357–361 (2012).
- 3 K.K. Chawla, *Composite Materials*, 3rd ed. Springer, New York, 2012.
- 4 J.Y. Lao, W.Z. Li, J.G. Wen, and Z.F. Ren, "Boron carbide nanolumps on carbon nanotubes," *Appl. Phys. Lett.*, **80** [3] 500–502 (2002).
- 5 A.C. Dupuis, "The catalyst in the CCVD of carbon nanotubes-a review," *Prog. Mater. Sci.*, **50** [8] 929–961 (2005).
- 6 Y. Li, J. Liu, Y. Wang, and Zhong Lin Wang, "Preparation of monodispersed Fe-Mo nanoparticles as the catalyst for CVD synthesis of carbon nanotubes," *Chem. Mater.*, **13** [3] 1008–1014 (2001).
- 7 A. V Melezhyk, Y.I. Sementsov, and V. V Yanchenko, "Synthesis of fine carbon nanotubes co-deposited at metallic oxide catalysts," *Appl. Chem. (in Russ.)*, **78** [6] 938–943 (2005).
- 8 A. Barreiro, S. Hampel, M.H. Rummeli, C. Kramberger, A. Grneis, K. Biedermann, A. Leonhardt, T. Gemming, *et al.*, "Thermal decomposition of ferrocene as a method for production of single-walled carbon nanotubes without additional carbon sources," *J. Phys. Chem. B*, **110** [42] 20973–20977 (2006).
- 9 R.H. Woodman, B.R. Klotz, and R.J. Dowding, "Evaluation of a dry ball-milling technique as a method for mixing boron carbide and carbon nanotube powders," *Ceram. Int.*, **31** [5] 765–768 (2005).
- 10 C. Singh, M.S.P. Shaffer, and A.H. Windle, "Production of controlled architectures of aligned carbon nanotubes by an injection chemical vapour deposition method," *Carbon N. Y.*, **41** [2] 359–368 (2003).
- 11 T.S.R.C.M. A. K. Suri, C. Subramanian, J. K. Sonber, "Synthesis and consolidation of boron carbide: a review," *Int. Mater. Rev.*, **55** [1] 4–40 (2010).